A quantitative FLASH effectiveness model to reveal potentials and pitfalls of high dose rate proton therapy

Miriam Krieger[1,2] | Steven van de Water[2] | Michael M. Folkerts[3] | Alejandro Mazal[4] | Silvia Fabiano[2,5,6] | Nicola Bizzocchi[2] | Damien C. Weber[2,6,7] | Sairos Safai[2] | Antony J. Lomax[2,5]

[1] Varian Medical Systems Particle Therapy GmbH & Co. KG, Troisdorf, Germany

[2] Center for Proton Therapy, Paul Scherrer Institute, Villigen, Switzerland

[3] Varian Medical Systems, Inc., Palo Alto, California, USA

[4] Centro de Protonterapia Quironsalud, Madrid, Spain

[5] Department of Physics, ETH Zurich, Zurich, Switzerland

[6] Department of Radiation Oncology, University Hospital Zurich, Zurich, Switzerland

[7] Department of Radiation Oncology, Inselspital, Bern University Hospital, University of Bern, Bern, Switzerland

Correspondence
Miriam Krieger, Center for Proton Therapy, Paul Scherrer Institute, Forschungsstrasse 111, 5232 Villigen, Switzerland.
Email: Miriam.krieger@psi.ch

Miriam Krieger and Steven van de Water shared first authorship.

Abstract

Purpose: In ultrahigh dose rate radiotherapy, the FLASH effect can lead to substantially reduced healthy tissue damage without affecting tumor control. Although many studies show promising results, the underlying biological mechanisms and the relevant delivery parameters are still largely unknown. It is unclear, particularly for scanned proton therapy, how treatment plans could be optimized to maximally exploit this protective FLASH effect.

Materials and Methods: To investigate the potential of pencil beam scanned proton therapy for FLASH treatments, we present a phenomenological model, which is purely based on experimentally observed phenomena such as potential dose rate and dose thresholds, and which estimates the biologically effective dose during FLASH radiotherapy based on several parameters. We applied this model to a wide variety of patient geometries and proton treatment planning scenarios, including transmission and Bragg peak plans as well as single- and multifield plans. Moreover, we performed a sensitivity analysis to estimate the importance of each model parameter.

Results: Our results showed an increased plan-specific FLASH effect for transmission compared with Bragg peak plans (19.7% vs. 4.0%) and for single-field compared with multifield plans (14.7% vs. 3.7%), typically at the cost of increased integral dose compared to the clinical reference plan. Similar FLASH magnitudes were found across the different treatment sites, whereas the clinical benefits with respect to the clinical reference plan varied strongly. The sensitivity analysis revealed that the threshold dose as well as the dose per fraction strongly impacted the FLASH effect, whereas the persistence time only marginally affected FLASH. An intermediate dependence of the FLASH effect on the dose rate threshold was found.

Conclusions: Our model provided a quantitative measure of the FLASH effect for various delivery and patient scenarios, supporting previous assumptions about potentially promising planning approaches for FLASH proton therapy. Positive clinical benefits compared to clinical plans were achieved using hypofractionated, single-field transmission plans. The dose threshold was found to be an important factor, which may require more investigation.

KEYWORDS
effectiveness model, FLASH, scanned proton therapy

1 | INTRODUCTION

FLASH radiotherapy has gained increasing interest in recent years. Many studies have shown a protective, so-called "FLASH" effect on healthy tissues without compromising tumor control for dose delivered orders of magnitude faster than in conventional radiotherapy.

In 2014, Favaudon et al. found that mice irradiated with electron beams at dose rates >40 Gy/s did not show any lung fibrosis, whereas the same dose levels delivered at 0.03 Gy/s induced substantial fibrosis.[1] Importantly, no dose rate-dependent difference in the tumor control was observed.

Since then, many other studies have confirmed the protective effects on a variety of healthy tissue types and preclinical models.[2–10]

In these studies, the delivery physics is central to the experimental setup and discussion. Although the initial publication of Favaudon et al. focused on 40 Gy/s, it is not clear where in the FLASH dose rate range this value falls. Some studies regard 40 Gy/s as a minimum threshold for observing the FLASH effect,[5] whereas others suggest that 100 Gy/s is the minimum.[4] Even the very definition of dose rate is a point of discussion, as some authors highlight the importance of the instantaneous dose rate within the pulsed microstructure of the radiofrequency (RF) beam delivery system,[11] whereas the often-reported value (like 40 Gy/s) is the time-averaged dose rate. Other studies suggest the presence of a minimum dose threshold to trigger the FLASH effect.[7]

The search for a biologically meaningful dose and dose rate definition gains even more importance for pencil beam scanned (PBS) proton therapy, where a narrow proton beam is scanned spot by spot to cover the whole target, giving rise to a spatially and temporally varying dose rate. Several groups attempted to quantify the dose rate in order to estimate the potential magnitude of the FLASH effect for certain PBS treatment plans. Van de Water and colleagues introduced the "Dose-Averaged Dose Rate" (DADR), calculating the voxel-wise instantaneous dose rate of every spot and taking the dose-weighted average of these dose rates.[12] The "Spot-Peak Dose Rate" analysis presented by Van Marlen et al.[13] goes one step further and differentiates between spot-wise dose rates to calculate the voxel-wise percentage of the total dose that is delivered above a certain threshold dose rate. Although these dose rate metrics can give a first-order estimate of the dose rates correlated to a certain treatment plan, they ignore the dead times in-between spots needed to scan the beam laterally or change the beam energy. A different dose rate definition that overcomes this limitation is the "PBS dose rate" recently presented by Folkerts et al.[14] This metric includes the dead times in the voxel-wise average dose rate, while excluding the time before the first and after the last dose contribution to a given voxel. Although this PBS dose rate correlates more closely with the field-averaged dose rates reported in electron FLASH literature than DADR, it does not differentiate between spots that are delivered at different instantaneous dose rates, and thus the dose in any voxel is assumed to either be delivered fully as FLASH, or with no FLASH at all when simply assuming a dose rate threshold.

Until the biological mechanisms behind the FLASH effect are better understood, the proper definition of dose rate will remain elusive. This study attempts to sidestep this issue by instead introducing a phenomenological FLASH effectiveness model. Our model is based on the idea of Mazal et al.,[15] who suggested the use of an effectiveness factor for the contribution of every pencil beam to every voxel: this factor takes a value <1 if a certain portion of dose is delivered as FLASH, and equal to 1 otherwise. This concept allows the estimation of the potential biologically effective dose reduction for highly variable treatment deliveries, common to intensity-modulated proton therapy (IMPT). In order to determine what dose is delivered as FLASH, our extended model incorporates four parameters: a dose threshold, a dose rate threshold, a FLASH effectiveness factor, and a persistence time within which FLASH is still considered active after the FLASH trigger window has ended. In contrast to the previously mentioned dose rate definitions, this model includes basic radiobiological considerations, without making assumptions about the underlying biological mechanisms.

The aim of the current study, focused on PBS proton delivery, is to quantify the potential FLASH effect for a variety of treatment sites using different treatment planning and delivery strategies, and additionally to assess the FLASH sparing dependence on physical characteristics such as dose rate and dose thresholds as well as the persistence time. In addition, we compare any potential dosimetric benefits of FLASH proton therapy with current clinical practice. To this purpose, we present a FLASH effectiveness model, which combines representative PBS delivery dynamics with a parametrized implementation of the aforementioned physical parameters allowing for a survey of high dose rate PBS proton treatment plans. Because the only biology assumed is a FLASH sparing "factor," and all physical variables are parameterized, this model enables the creation of candidate FLASH treatment plans based on realistic delivery parameters available clinically today, and as such could help guide future biology research aimed at clinical translation of proton FLASH therapy.

2 | MATERIALS AND METHODS

2.1 | FLASH effectiveness model

The FLASH effectiveness model attempts to consider experimental observations to calculate the biologically
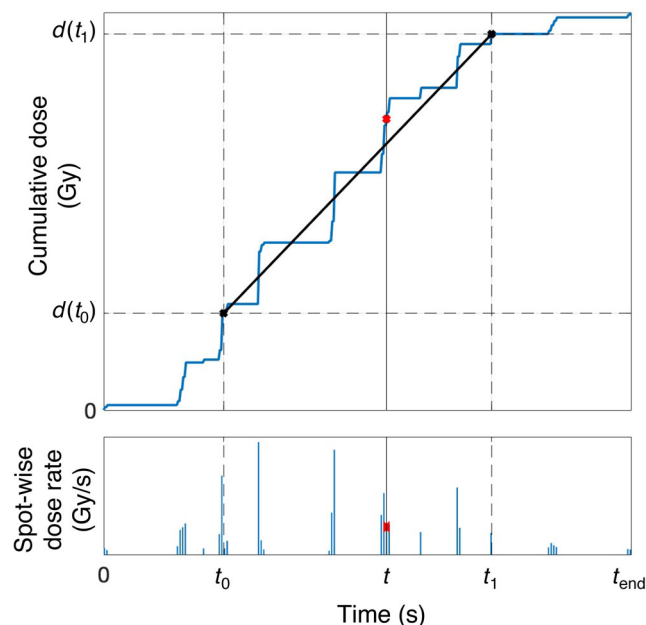
FIGURE 1 Illustration of the procedure of determining whether the dose delivered at time t (red marker) is delivered in FLASH mode (top panel). If the average dose rate and the total dose delivered between any $t_0 \leq t$ and $t_1 \geq t$ (black markers) are above the respective thresholds, FLASH is triggered at time t. Bottom panel: spot-wise dose rate that defines the given cumulative dose

effective dose in the presence of the FLASH effect. The idea was first presented by Mazal et al.[15] and implemented in MATLAB (version 2018a) for this work. The principle is the following: if the time varying dose rate and dose to a voxel are above the respective thresholds, FLASH is "triggered" for that voxel. Once triggered, the FLASH effect will remain "active" within this voxel for a certain period of time, known as the *persistence time*. Any dose delivered as FLASH is assumed to be biologically less "effective" and thus multiplied by a FLASH effectiveness factor (FEF) that is <1 (correlating to the reduced toxicity). Because the FLASH effect only affects healthy tissue cells without altering the tumor response, the model assigns this factor only to healthy tissues, while keeping the dose in tumor cells unchanged (i.e., FEF = 1). Details of the algorithm follow.

2.1.1 | Triggering FLASH

For every voxel v, consider the cumulative dose delivered as a function of time, $d_v(t)$ (see Figure 1). In a PBS delivery, multiple temporally and spatially separated pencil beams will contribute to $d_v(t)$. All pencil beams contributing to the respective voxel are delivered between t_{start} and t_{end}. For every time point t between t_{start} and t_{end} with nonzero dose contribution, FLASH is triggered if there exist t_0 and t_1 with $t_{start} \leq t_0 \leq t \leq t_1 \leq$

t_{end}, which fulfil the following two conditions:

$$\frac{d_v(t_1) - d_v(t_0)}{t_1 - t_0} \geq DR_{thr},$$

$$d_v(t_1) - d_v(t_0) \geq D_{thr},$$

where DR_{thr} describes the dose rate threshold and D_{thr} is the dose threshold. In other words, FLASH is triggered for any time point during the dose delivery if there is a time window around this time point within which the average dose rate including any dead times is above the dose rate threshold and the total dose delivered is above the dose threshold. This definition may result in multiple FLASH trigger windows per treatment field. Each of those FLASH trigger windows is followed by a persistence time, within which the FLASH effect is still considered active, regardless of the dose or dose rate delivered in this period. The FLASH trigger itself is independent of the persistence time. More information on how the time points t_0 and t_1 are determined can be found in the Supporting Information.

2.1.2 | Parameters

The above-presented model includes four main parameters: the dose threshold D_{thr}, the dose rate threshold DR_{thr}, the FLASH persistence time, and the FEF. Although the FEF only scales the magnitude of the FLASH-induced dose reduction linearly, the other three parameters influence the spatiotemporal FLASH distribution in a nontrivial way. The FLASH persistence time could be interpreted as reoxygenation time in case the oxygen depletion hypothesis proves true but is also a valid FLASH-prolonging parameter in the case of different biological mechanisms.

Based on the publication of Pratx et al., an FEF of 0.67 was chosen for this study, allowing for a maximal sparing of 33%.[16] Favaudon et al.[1] and Montay-Gruel et al.[4] have observed the FLASH effect for dose rates above 40 and 100 Gy/s, respectively, which were assumed as potential thresholds in this study. The dose threshold is currently less well-explored. Some studies, however, suggested a value of 5–10 Gy.[1,4] Lastly, the FLASH persistence time is estimated to be in the range of 200–500 ms.[16]
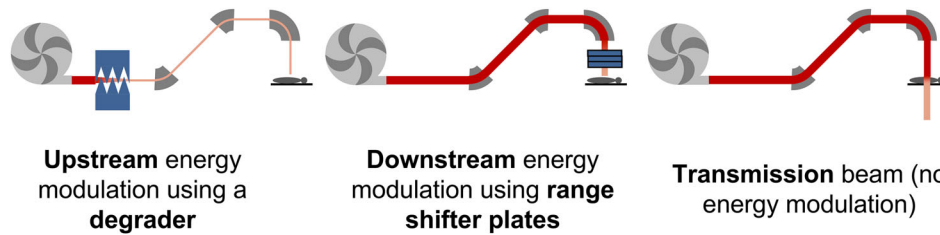
2.2 | Treatment planning scenarios and anatomical sites

Several treatment planning strategies were evaluated in this study, as summarized in Table 1. Three major characteristics were varied: (i) which part of the proton pencil beam is used to cover the tumor, that is, conventional

TABLE 1 Overview over the different treatment planning scenarios

Plan name	Mode	Energy modulation	Number of fields
Single field upstream (SU)	Bragg peak	Upstream	1
Multifield upstream (MU, clinical reference plan)	Bragg peak	Upstream	2–4
Single field downstream (SD)	Bragg peak	Downstream	1
Multifield downstream (MD)	Bragg peak	Downstream	2–4
Single field transmission (ST)	Transmission	None	1
Multifield transmission (MT)	Transmission	None	7–11

Note: Number of fields of the MU/MD plans: 2 (pancreas, prostate, lung), 3 (brain), and 4 (nasal cavity). Number of fields for the MT plans: 7 (PR1), 9 (PA1/2, LU1, NC1), 10 (BR1, NC2, PR2), and 11 (BR2, LU2).

Upstream energy modulation using a **degrader**

Downstream energy modulation using **range shifter plates**

Transmission beam (no energy modulation)

FIGURE 2 Illustration of the three delivery techniques considered in this study

Bragg peak based versus transmission/shoot-through planning; (ii) whether the beam energy is modulated using a conventional upstream degrader or downstream range-shifter plates close to the patient; and (iii) the number of fields per plan. Each of these characteristics affects the total dose per spot as well as the delivery dynamics and thus may influence the FLASH effect. The difference between upstream- and downstream-modulated plans were simulated because high energies are generally transported more efficiently (see Section 2.3), which renders downstream energy modulation using range-shifter plates an interesting approach.[17] Please note that the range-shifter plates were modeled by adjusting the water equivalent depth of each voxel in steps of 4.6 mm, which in turn increased the spot sizes at the target position compared to upstream-degraded plans due to increased multiple coulomb scattering. The difference between upstream and downstream energy modulation as well as transmission planning is illustrated in Figure 2.

All treatment plans were generated using an in-house-developed planning system based on the open-source planning toolkit "matRad."[18] Multifield plans were optimized using IMPT,[19] whereas transmission plans only contained pencil beams with the highest available beam energy of 229 MeV. Spot widths (sigma, in-air at isocenter, without pre-absorber) ranged approximately between 5.2 and 2.3 mm for energies of 71 and 229 MeV, respectively. Please note that no air gap was modeled, representing a best-case scenario for the range shifter plans in terms of spot sizes and thus of plan quality and integral dose. In order to remove low-weighted spots and potentially increase the dose rate, the number of spots

in all treatment plans was greatly reduced by applying the spot-reduction algorithm presented by Van de Water et al.[20]

Treatment plans were generated for five different treatment sites: brain (BR), lung (LU), nasal cavity (NC), pancreas (PA), and prostate (PR). Each of these five treatment sites is represented in this study by two separate patient geometries, that is, 10 geometries were investigated in total. To facilitate practical comparison between treatment sites, all cases were planned with a prescribed dose of 60 Gy, delivered in 30 fractions, irrespective of the dose that was prescribed clinically. We used prioritized multicriterial optimization, aiming first at adequate target coverage ($V_{95\%} \geq 98\%$) and target homogeneity ($V_{107\%} \leq 2\%$), followed by improving dose conformality (using ring structures around the target volume) and reduction of OAR doses. If a clinical treatment plan was available (for the brain, lung, nasal cavity, and pancreas cases), the (scaled) clinical OAR doses were set as planning goal, otherwise OAR doses were minimized as much as possible (for the prostate cases).

The single-field beam angles were selected manually, generally trying to avoid normal tissue exposure as much as possible. For the multifield Bragg peak-based plans, the original clinical field arrangements were used if available, with the exact number of fields depending on the treatment site: two fields for the pancreas and lung cases, three fields for the brain cases, and four fields for the nasal cavity cases. For the prostate cases, a typical two-field lateral parallel-opposed arrangement was applied. Multifield transmission planning was initiated with a 120-field arrangement, distributed over three noncoplanar arcs (–30, 0, and 30 degrees with

respect to transverse plane, 9-degree field separation within each arc) for the brain, nasal cavity, and pancreas cases, or distributed over a single coplanar arc (3-degree field separation) for the lung and prostate cases to avoid fields entering via the arms or legs. Fields were subsequently excluded in an iterative fashion until further exclusion would result in deterioration of dosimetric plan quality, resulting in seven to 11 transmission fields remaining in the plan depending on the case. This approach was similar to the energy layer-reduction technique described previously.[21]

All such FLASH planning scenarios were compared to standard, but spot-reduced, multifield Bragg peak-based plans with upstream energy modulation using the original clinical field arrangements as a reference in terms of dose to healthy tissue.

2.3 | Delivery dynamics

All simulations were performed for the delivery dynamics of representative clinical proton scanning gantry. We considered a theoretically achievable beam intensity, neglecting any safety or monitoring restrictions. The maximum beam intensity at isocenter as a function of energy ranged between 5.0×10^9 and 1.2×10^{12} protons per second for energies of 71 and 229 MeV, respectively, as shown in figure S2 of Van de Water et al.,[12] assuming a cyclotron current of 800 nA and considering the transmission of the beamline and the gantry for each proton energy.[22,23] Furthermore, it was assumed that the intensity of the beam could be varied spot wise, ensuring a minimum spot duration of 3 ms. Lateral scanning between the spots was assumed to take 3 ms and the energy switching times were 250 and 50 ms for upstream and downstream energy modulation, respectively. Every field was considered separately, that is, the time between fields was assumed to be much greater than the persistence time and the trigger windows were restricted to one field at a time.

2.4 | Analysis

The voxel-wise FLASH dose, or FEF-weighted dose $D_{v,FEF}$, was calculated using the following formula:

$$D_{v,FEF} =$$

$$\sum_t \left(d_v(t) \cdot \begin{cases} (1 - FEF), & \text{if } d_v(t) \text{ delivered as FLASH} \\ 1, & \text{else} \end{cases} \right),$$

with $d_v(t)$ being the dose delivered to voxel v at time t.

The FLASH effect for a plan p was then quantified using two figures of merit: the relative reduction of the integral dose ΔID and the relative reduction of the mean dose in the margin around the gross tumour volume that defines the planning target volume (GTV-to-PTV margin) ΔMD due to the FLASH effect:

$$\Delta ID(p) = \left(1 - \frac{ID_{FLASH}(p)}{ID_{Phys}(p)} \right) \times 100\%$$

$$\Delta MD(p) = \left(1 - \frac{MD_{FLASH}(p)}{MD_{Phys}(p)} \right) \times 100\%,$$

where the subscripts "FLASH" and "Phys" refer to the FEF-weighted and the physical dose distributions, respectively. In addition, the clinical benefit CB of FLASH was quantified in terms of the difference between the FEF-weighted integral dose of each plan and the physical integral dose of the clinical reference plan Ref:

$$CB(p) = \left(1 - \frac{ID_{FLASH}(p)}{ID_{Phys}(Ref)} \right) \times 100\%.$$

The integral dose ID was calculated as the sum of the dose of all dose-receiving voxels outside the PTV. The clinical benefit was defined using the integral dose rather than using organ doses because of its independence of the specific beam arrangement and because of its applicability to a broad variety of treatment sites.

The analysis of this study was split into three parts. First, the magnitude of the FLASH effect was investigated using all planning approaches listed in Table 1 for one pancreas patient (PA1), together with a specific set of simulation parameters: 5 Gy dose threshold, 40 Gy/s dose rate threshold, 0.67 FEF, 200 ms persistence time, and a fraction dose of 22.3 Gy (explained below). This part of the analysis was used to determine the most promising planning scenarios and exclude plans with no substantial FLASH effect from further analysis. Second, the two most promising planning scenarios (i.e., single-field downstream energy-modulated, single-field transmission) were investigated for all 10 patient datasets and for the same simulation parameters mentioned above in order to identify any dependence of the FLASH effect on the treatment site. Lastly, because the correct values of the simulation parameters are unknown, a sensitivity analysis was performed to identify which parameters influence the magnitude of the modeled FLASH effect most. The analysis was done in a one-at-a-time fashion, neglecting any inter-parameter correlations, varying the dose threshold, the dose rate threshold, the persistence time, and the dose per fraction separately around their respective reference values of 5 Gy, 40 Gy/s, 200 ms, and 22.3 Gy/fx. The considered parameter ranges were 0–25 Gy, 40–520 Gy/s, 0–500 ms, and 4.8–22.3 Gy/fx. The values for the dose per fraction were chosen to be biologically equivalent to a reference fractionation of 30×2 Gy using a tumor α/β ratio of 10 Gy and assuming treatments with one to 10 fractions.
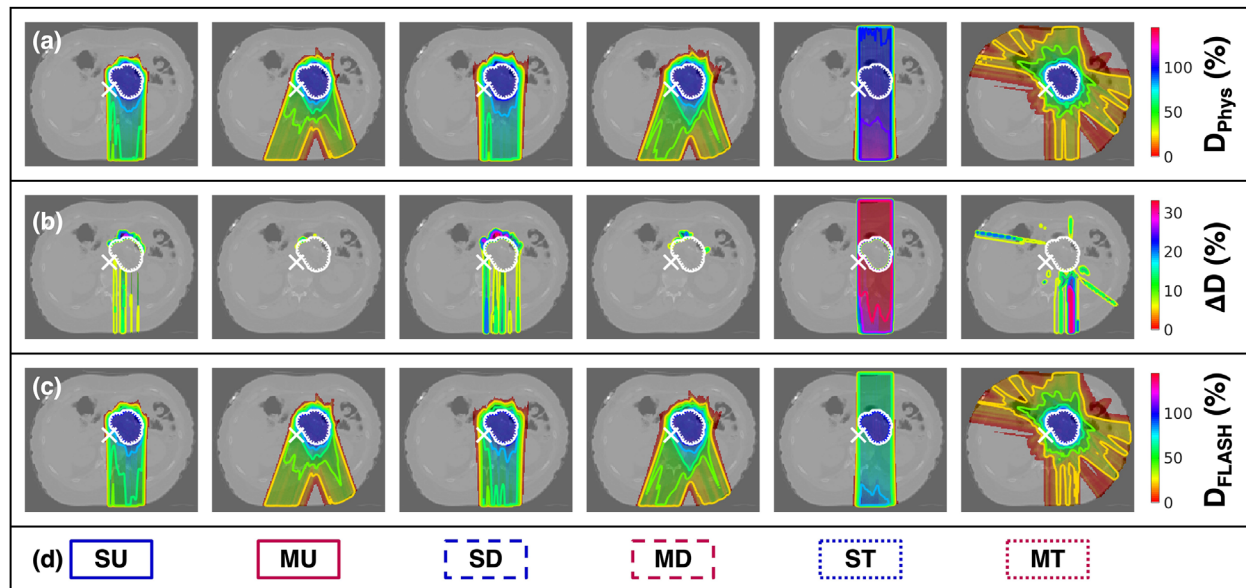
FIGURE 3 Example dose distributions showing all planning strategies for the pancreas case PA1. The considered parameters were 22.29 Gy fraction dose, 5 Gy dose threshold, 40 Gy/s dose rate threshold, and 200 ms persistence time. (a) Physical dose distributions, given in percent of the prescribed dose. (b) Voxel-wise FLASH effect given as the effective dose reduction relative to the respective voxel dose. Note that no reduction is shown within the GTV, because it mainly consists of tumor cells, which are assumed not to be subject to FLASH. (c) FEF-weighted dose, given in percent of the prescribed dose. (d) Plan descriptions. S, single-field plan; M, multi-field plan; U, upstream energy modulation; D, downstream energy modulation; T, transmission (no energy modulation). FEF, FLASH effectiveness factor

3 | RESULTS

3.1 | Detailed analysis of one pancreas patient

To illustrate the respective treatment plans, Figure 3a shows an example slice through the dose distributions for all planning scenarios for pancreas patient PA1. Identical field arrangements were chosen for upstream and downstream energy modulation, as was the case for all patients. The voxel-wise FLASH dose reduction is depicted in subfigure (b) as a percentage of the physical voxel dose, assuming the reference FLASH model parameters. Please note that no dose reduction is shown inside the GTV because tumor cells were assumed not to be affected by FLASH. All plans exhibited some FLASH, with the lowest amount of FLASH seen for multifield Bragg peak plans. For Bragg peak-based plans, FLASH mainly occurred in the entrance region and at the distal end of a field. For the single-field transmission plan, however, FLASH was observed along the full beam path. The FEF-weighted dose distributions are presented in Figure 3c. A similar overview for all patients can be found in Figure S1.

A quantitative analysis of the FLASH effect in PA1 is presented in Figure 4. The FEF-weighted dose volume histograms for the GTV-to-PTV margin in comparison to the non-FEF-weighted clinical reference plan are shown in Figure 4a. The margin volume is of particular interest because it is a high-dose region that poten-

tially consists of both healthy tissue and tumor cells. Under the assumption that the FLASH effect works on a cellular level, a potential differential response would be most pronounced and clinically interesting in the margin. Note that the margin is part of the PTV, indicating that the physical (non-FEF-weighted) dose within this region was nearly identical for all plans. In addition, Figure 4c shows the reduction in FEF-weighted integral dose for all planning scenarios separately. Figures 4a and 4c show that there was more FLASH dose reduction for single-field plans (blue) than for multifield plans (red), with an average ΔID of 14.7% and 3.7% over the three delivery scenarios, respectively. Transmission plans (dotted) resulted in substantially higher FLASH effects than downstream (dashed) or upstream (solid) modulated plans, with ΔID of 19.7%, 4.8%, and 3.1%, respectively, when averaged over single and multifield plans. Comparing the FEF-weighted ID of any plan to the physical ID of the clinical reference plan, as quantified by the clinical benefit and plotted in Figure 4d, paints a different picture. Single-field plans showed a higher clinical benefit than multifield plans with average CB numbers of −10.3% and −36.6%, respectively, when averaged over all delivery scenarios. This is partly due to the chosen shorter path lengths of single-field plans compared to the clinical plan. However, only upstream-modulated plans showed a positive CB (6.2%), with downstream-modulated and transmission plans having reduced mean CBs of −21.6% and −54.9%, respectively. This indicates that the increased physical dose conformation provided by the
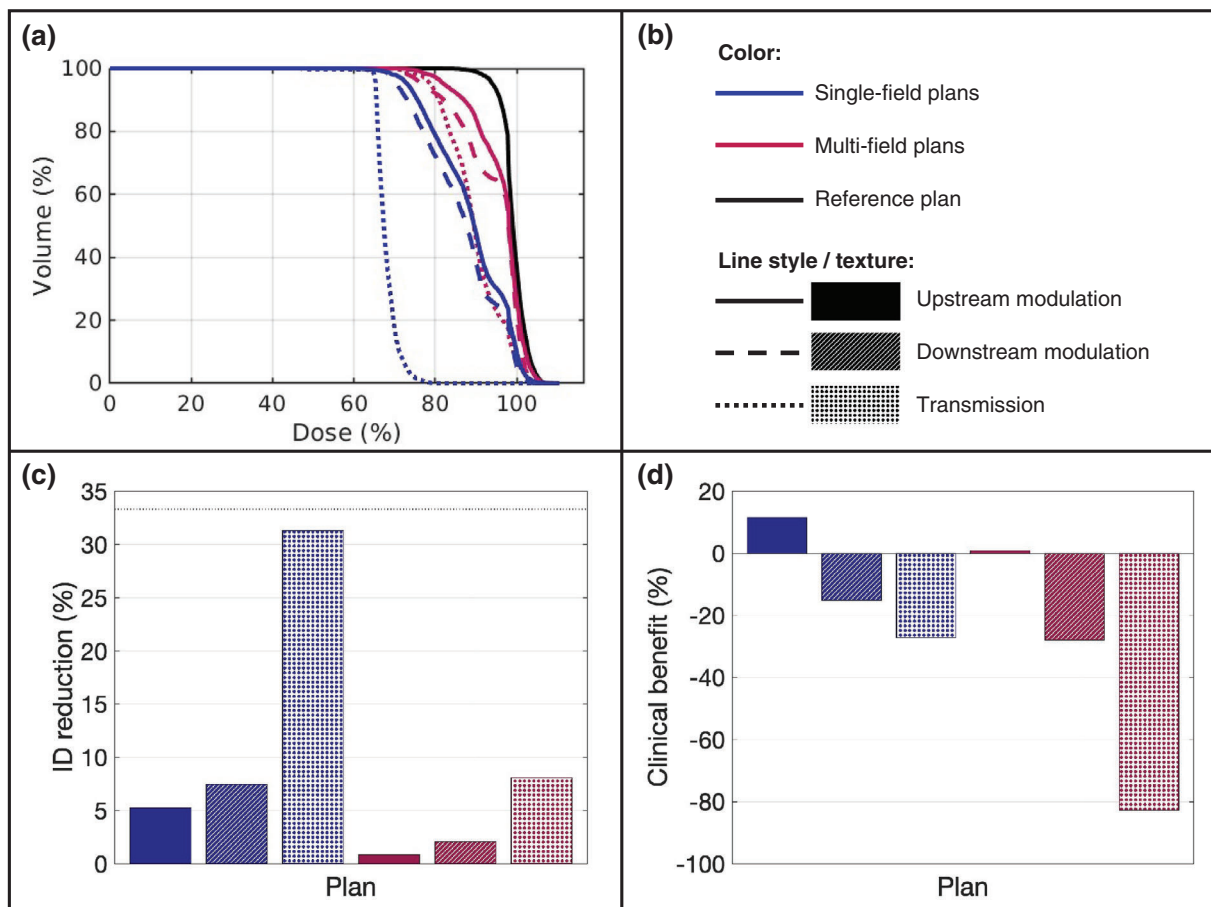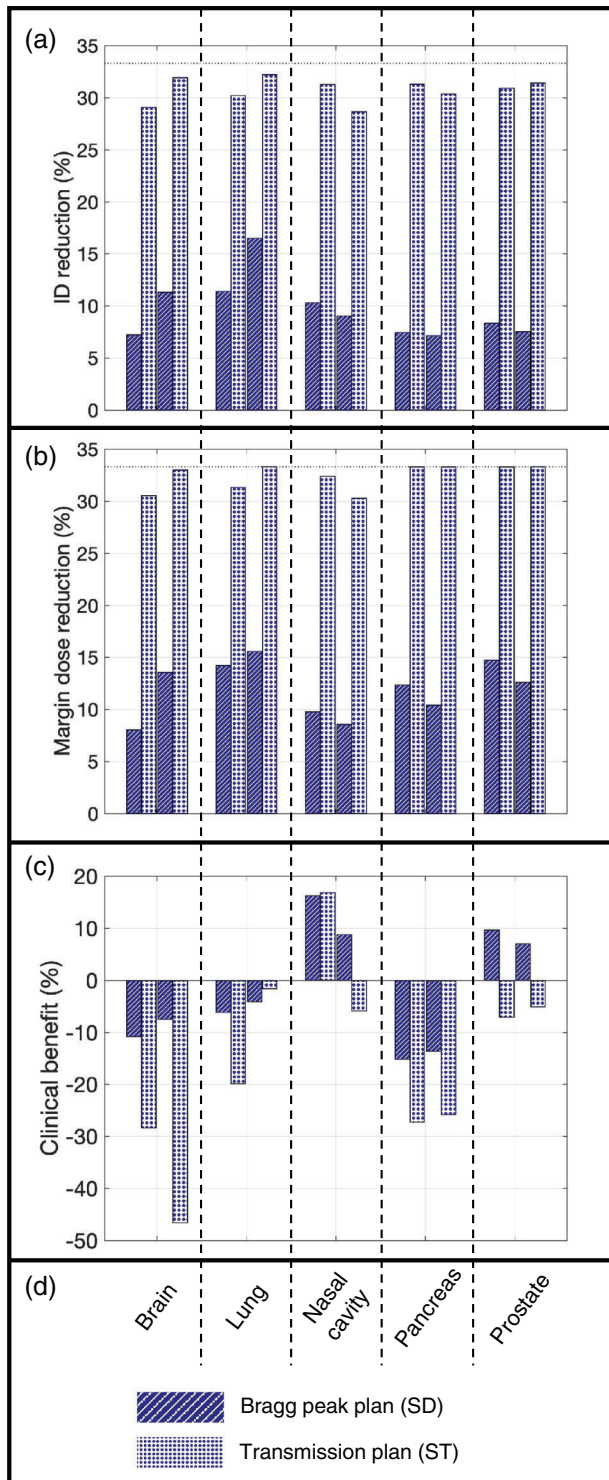
FIGURE 4 Comparison of the magnitude of the FLASH effect for the different planning approaches for the pancreas case PA1. The considered parameters were 22.29 Gy fraction dose, 5 Gy dose threshold, 40 Gy/s dose rate threshold, and 200 ms persistence time. Note that the clinical reference plan is a multifield, upstream-modulated plan, that is, it corresponds to the red solid plots when considering the FLASH-weighted dose. (a) DVHs of the GTV-to-PTV margin for all planning scenarios. The red and blue curves indicate the FEF-weighted doses, whereas the black curve shows the physical (non-FEF-weighted) dose of the clinical reference plan as a comparison. (b) Legend of the colors and of the different line styles (for [a]) and face textures (for [c] and [d]). (c) Reduction of the integral dose induced by the FLASH effect for every plan separately. Bars close to zero indicate little FLASH, whereas bars close to 33% present near-maximum FLASH. (d) Clinical benefit of each FEF-weighted plan compared to the clinical physical reference plan. Positive values indicate less FEF-weighted integral dose for the respective plan than for the non-FLASH-weighted clinical plan. DVH, dose volume histogram; FEF, FLASH effectiveness factor

upstream modulation outweighs the increased FLASH effects resulting from either dowstream modulation or transmission.

As such, and to reduce the data load, the further analysis focussed on the two planning strategies that proved most promising to induce substantial FLASH effects without compromising the clinical benefit much—single-field transmission (ST) and single-field, downstream energy modulation (SD). The single-field, upstream enegery modulation plan (SU), despite providing a higher clinical benefit than the SD plan, was not chosen because its clinical benefit originates from the plan conformality rather than the FLASH effect. Although the results for all the plans have only been shown for one specific patient, the same conclusions can be drawn for all 10 patients (see Figure S2).

3.2 | FLASH at different tumor sites

The magnitude of the FLASH effect is compared for different treatment sites in Figure 5 for the ST and SD plans. The plots contain the results for two patients per site as indicated by the two separate bars per plan and site. For the transmission plan (ST), the ΔID of all patients was 30.8(1.2)%, given as mean(standard deviation). Similar values were found for the margin dose reduction ΔMD, averaging 32.4(1.2)%. As already found for the single pancreas case, the ID and margin mean dose reduction for the downstream-modulated Bragg peak plan (SD) were substantially lower than for the transmission plan in all patients, averaging 9.6(2.9)% and 12.0(2.6)%, respectively. Although the magnitudes of the FLASH effect within one plan were comparable among all patients, the clinical benefit of each plan,

FIGURE 5 Comparison of the magnitude of the FLASH effect for five different treatment sites with two patients each and the two selected planning strategies. (a) FLASH effect in terms of integral dose reduction for each plan separately. (b) FLASH effect in terms of mean dose reduction within the GTV–PTV margin. (c) Clinical benefit of each FEF-weighted plan compared to the clinical physical reference plan. Positive values indicate a lower FEF-weighted integral dose for the respective plan than for the non-FEF-weighted clinical plan. (d) Legend for subfigures (a) to (c). FEF, FLASH effectiveness factor

given by −15.1(18.0)% and −1.6(11.1)% for the transmission and Bragg peak plans, respectively, varied drastically, as reflected by the large standard deviation. For the given reference FLASH parameters, the nasal cavity and prostate cases were the only sites that presented a positive clinical benefit for the SD plans, whereas for the ST plans, only the NC1 case showed a positive clinical benefit. For the brain, lung, and pancreas cases, the clinical benefit was negative for both planning scenarios.

Please note that the interpatient variability in ID or margin mean dose reduction was also limited for the plans not shown in this section, whereas the clinical benefit was strongly patient dependent. Corresponding diagrams can be found in Figure S3.

For easier comparisons among different treatment sites, the analyses were performed using the integral dose definition. The interested reader will find data on specific organs at risk in Figure S4.

3.3 | Sensitivity analysis

Figure 6a shows the dependence of the FLASH effect on dose per fraction, dose threshold, dose rate threshold, and persistence time in terms of ΔID for the ST and the SD plans, with ID reduction varying between 0% (no FLASH effect) and 33% (all dose delivered as FLASH, using an FEF of 0.67). Given the reference parameters, the magnitude of the FLASH effect strongly depends on the dose per fraction and the threshold dose (upper row in Figure 6a), with high fraction doses and low dose thresholds inducing most FLASH. This was particularly pronounced for the transmission plans, which showed a substantial FLASH effect already for the reference parameters. It is worth pointing out that for most patients, the ST plan induced high FLASH effects for a threshold dose up to close to the fraction dose, at which a sudden drop occurred (top right plot). For the SD plan, a similar drop occurred at much lower dose thresholds. A rather continuous decline of the FLASH effect was found as a function of increasing dose rate thresholds for both scenarios, as seen in the bottom left plot. Lastly, as indicated by the bottom right, the FLASH effect was found to be largely independent of the persistence time for either planning approach.

The clinical benefit of both planning approaches, illustrated in Figure 6b, revealed the same overall trends that were described above. Because a relatively broad variety of clinical benefits among the different patients had been found at the reference parameters, it is not a surprise that the clinical benefit data showed a wider spread than the ID reduction also when varying the parameters one at a time, resulting in the broader bands in Figure 6b compared with Figure 6a.
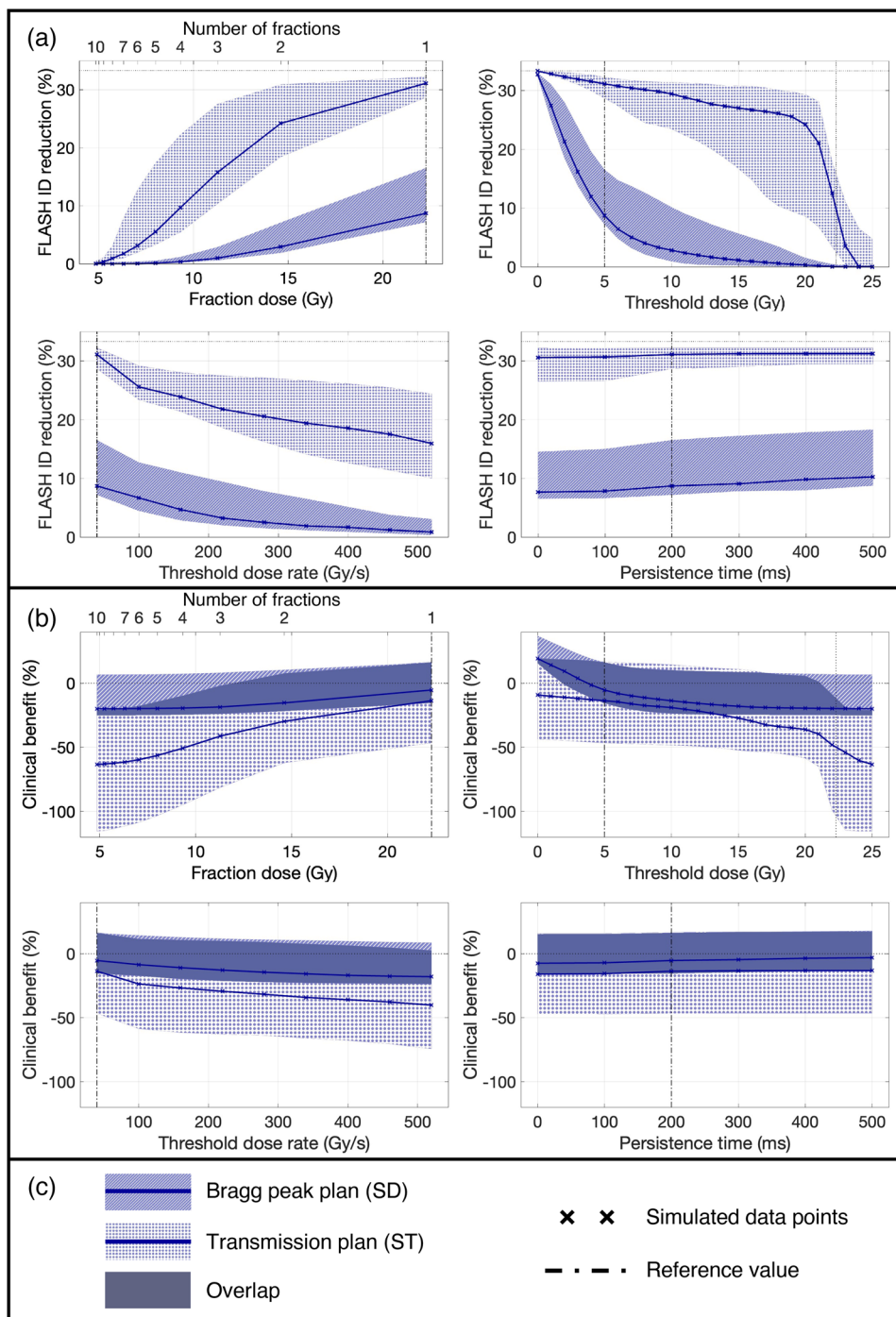
FIGURE 6 Sensitivity analysis of the FLASH effect for varying parameter values. The shaded bands include all 10 patients for the single-field transmission plan (dotted) and the single-field, downstream-modulated Bragg peak plan (ruled). The solid line describes the median. The dashed-dotted line indicates the reference value of each parameter. The dotted lines in the upper right plots additionally indicate the fraction dose as a reference. (a) Reduction in integral dose within one plan due to FLASH. Low values indicate little FLASH, whereas 33% (dotted line) describes a maximally possible FLASH effect. (b) Clinical benefit of each plan compared to the clinical reference plan (MU). Positive values indicate a lower integral dose of the respective FEF-weighted plan compared to the non-FEF-weighted clinical reference plan, thus showing a potential clinical benefit. (c) Legend for both (a) and (b). FEF, FLASH effectiveness factor

4 | DISCUSSION

In this study, we utilized a novel FLASH effectiveness model to investigate the potential impact of various PBS delivery scenarios and model parameters on the FLASH effect. Based on our phenomenological description, we identified a larger magnitude of FLASH for fewer fields per plan and when applying transmission beams instead of exploiting the Bragg peak. The clinical benefit compared to a clinical reference plan, however, was more

favorable for Bragg peak plans than for transmission beams due to the latter's lower level of dose conformality. In addition, the clinical benefit varied greatly among different patient geometries and treatment sites. Lastly, the sensitivity analysis revealed that the FLASH effect most strongly depended on the fraction dose and dose threshold, with only a marginal influence of the persistence time. Our results show that some plans can potentially induce large FLASH effects; however, one must not forget about the pitfalls introduced by the, in some cases, considerably increased healthy tissue dose even after considering the FLASH dose reduction.

We would like to stress that our presented model is applicable regardless of the biological processes responsible for the FLASH effect. It is purely based on observations, such as the existence of dose and dose rate thresholds that were reported by several groups.[1,4,7] We do not claim to explain any of the underlying biological mechanisms but rather model the observed phenomena. In that sense, the persistence time built into our simulations is just another parameter to fit the model to observations and does not necessarily represent a reoxygenation time. Furthermore, this parameter was found to have only little impact on the FLASH effect, at least in the range investigated and for the considered reference parameters, which is why it could even be omitted to simplify the model without substantially affecting its accuracy. The main reason for the limited impact of the persistence time is that for the investigated plans, either most spots or only very few spots trigger FLASH in a voxel, which is why there are only a few spots that could profit from a persistence time. On the other hand, the model is easily adaptable to other parameters that will arise from a future better understanding of the FLASH effect.

Although a nonzero dose threshold was suggested by several experimental studies and would be supported by the oxygen hypothesis, we also performed simulations without any dose threshold. This allowed us to investigate the potential magnitude of the FLASH effect under the assumption that it is mediated by mechanisms that do not demand any dose threshold. Again, this strengthens our model by rendering it independent of the underlying, not yet fully understood biological processes.

Moreover, our study covered a wide range of potential dose thresholds in order to sensitize the community to this parameter's importance. Although many experiments focused on how the achievable dose rate affected FLASH,[1,4,7,9,24] only a few studies have investigated the dependence of the FLASH effect on the total delivered dose.[7,25] Our results indicate that the dose threshold is just as important as the dose rate threshold and thus should not be left out of consideration in future biological experiments. Indeed, depending on the fraction dose, the dose threshold may be the limiting factor for achieving FLASH.

Besides the apparent purpose of the dose threshold parameter, namely, the modeling of a potential biological dose threshold, it can additionally serve to tune the dose rate definition. The presented model uses a variable window width within which the dose rate as well as the dose itself need to be greater than their respective thresholds in order to trigger FLASH. On the one hand, by setting the dose threshold close to zero, the model tends to consider a smaller window size, and thus calculates the spot-wise dose rate, which is generally greater than an averaged dose rate that includes dead times. On the other hand, a dose threshold close to the maximum voxel dose inevitably increases the window size and as a consequence leads to an averaged dose rate definition that is similar to the PBS dose rate introduced by Folkerts and colleagues.[14] Because it is not currently known which kind of dose rate definition correlates most with the observed FLASH effects, such an additional dose rate tuner strengthens our model considerably.

Our simulations suggested that, within model assumptions and the investigated parameter space, substantial FLASH effects can only be observed in single-field transmission plans. The reasons for this are threefold. First, transmission plans lead to a much more homogeneous dose level along the entire beam paths compared to Bragg peak-based plans, meaning that the involved healthy tissues receive a dose close to the prescribed dose, which in turn increases the chance to exceed the threshold dose. Second, the transmission fields in our study consisted of a single energy layer, and as such had fewer spots with increased spot weight compared to the Bragg peak plans, which included many more spots in multiple energy layers. Because the minimum spot duration was assumed to be fixed (3 ms), the delivery of low-weighted spots necessitates a reduction of the beam current and thus the dose rate. And lastly, the transmission plans used only the highest available beam energy, that is, 229 MeV, which generally provided the highest beamline transmission efficiency. This was true for the downstream-modulated plans as well, because the beam energy was modulated just in front of the patient and thus only reduced the beam current marginally. This last point thus explains the differences in the predicted FLASH effects between upstream-modulated and transmission/downstream-modulated plans.

It is worth mentioning that for the Bragg peak plans, most FLASH was found at the distal end of each field. In our study, we did not model any linear energy transfer (LET) or relative biologal effectiveness (RBE) differences along the proton beam. The increased LET (and corresponding increased RBE) at the distal end of a treatment field, which partially falls onto healthy tissues, could be at odds with the beneficial FLASH effect. This potential loss of FLASH benefits is not present for transmission plans, because the high-LET regions lie outside of the patient. On the other hand, distal-end FLASH

effects could conversely help mitigate against such RBE effects.

The planning approach used in this study, namely, the spot-reduction algorithm, does not explicitly include the dose rate in the optimization process, but the increased dose rates are a consequence of the reduction of the number of spots. As such, it would not be straightforward to directly optimize the FLASH dose reduction using our framework. However, our presented FLASH effectiveness model is independent of the used optimizer, and thus it would be possible to include this model into the cost function of any other optimizer, resulting in a similar framework as the simultaneous dose and dose rate optimizer recently presented by Gao et al.[26]

In summary, our model is the first quantitative representation of previous findings, that is, that transmission plans and fewer treatment fields are likely to induce higher FLASH effects than conventional planning scenarios.[12] The sensitivity analysis additionally revealed that, in order to achieve a clinical benefit of the transmission plan compared to the clinical reference plan, hypofractionated treatments with increased fraction doses will be required. As an ancillary effect, this would also improve the patient comfort due to a considerably shorter treatment duration.

Our study was affected by certain limitations. First, we would like to mention that some assumptions about the machine characteristics are not currently clinically usable. The beam current was modeled in a way that is only restricted by physical limitations such as beam loss between the accelerator and the treatment isocenter. Any artificial beam current restrictions implemented for patient safety were ignored. Considering only clinically applied beam currents would result in lower dose rates and thus in lower FLASH effects. This is particularly true for transmission and downstream-modulated plans, which, in our study, fully exploited the higher, physically feasible beam currents. The same holds for our assumptions that the beam current could be varied spot by spot. A system where the beam current is varied, for instance, in-between energy layers would imply a change in dose rate for most spots to match the beam current for to the lowest weighted spot in each energy layer. In order to circumvent this issue, one would have to include the minimum spot weight per energy layer in the optimization process, as, for example, shown by Gao and colleagues.[27]

Moreover, our dose calculation algorithm did not model any air gap between the range-shifter plates and the patient surface in the downstream-modulated plans. The results presented in this study thus represent a setup where the range shifters are placed very close to the patient surface, which may not be feasible with current clinical machines.

Another point worth highlighting is that we based our selection of the most promising planning approaches on a certain set of reference parameters, and in particular

we assumed a nonzero dose threshold. This choice was based on several previously presented studies, which reported a FLASH effect only above a certain minimal dose.[7,25] It cannot be excluded, however, that there might be situations that do not present such a threshold. In the case of a 0 Gy dose threshold, the difference in ID reduction between the planning scenarios was found to be much smaller, whereas the differences in clinical benefit were comparable to the nonzero threshold results (data not shown here). This implies that for a 0 Gy dose threshold, Bragg peak-based planning scenarios would show FLASH effects that are comparable to transmission plans while providing a better dose conformality, thus becoming more clinically relevant. Furthermore, we assumed a general tumor alpha/beta ratio of 10 Gy for all tumor sites, whereas the actual number is clearly tumor specific. However, the alpha/beta ratio was only used to provide reasonable values for the fraction doses—our sensitivity analysis will provide an estimation of the expected FLASH effects for any desired fraction dose within the investigated range due to the rather monotonous dependence of the FLASH effect on the fraction dose.

Finally, in our FLASH effectiveness model, we considered all dose delivered within the FLASH triggering window and subsequent persistence time as FLASH dose, basically assuming FLASH to be triggered and to end instantaneously, as described by a step function. However, depending on the underlying biological mechanism, a more continuously varying FEF might provide a more appropriate description of the FLASH effect, and the model could be extended to also consider gradual variations in the FEF during dose delivery. On the one hand, such a varying FEF might lead to a lower FLASH effect because a part of the trigger dose would be weighted with a greater FEF. On the other hand, one could imagine that the FLASH trigger would be extended to include small dose contributions before what we considered to be the trigger window, and thus even increase the total FLASH effect.

To wrap up, we would like to state that we have left passive scattering out of consideration of this study on purpose. Our aim was to first compare Bragg peak to transmission planning in a comprehensive way for various treatment sites and for a broad range of parameters. Based on our findings, in our next study we will investigate how to exploit the conformality of Bragg peak-based plans while still achieving meaningful FLASH effect, for example, by means of passive scattering plans. Another delivery method to investigate is the use of range modulators in combination with a scanned beam, which provides increased dose rates due to the simultaneous delivery of an entire spread-out Bragg peak while maintaining the conformality of downstream energy modulated plans. The resulting FLASH effect is expected to be higher than for IMPT plans but potentially lower than for transmission plans.

5 | CONCLUSION

The FLASH effect varied among different planning scenarios and for different parameter values. Meaningful FLASH effects were found for single-field transmission plans in particular. In order to see a potential clinical benefit for those plans, hypofractionation schemes were required, because the FLASH effect was challenged by the reduced dose conformality compared to clinical IMPT plans. Further, the dose threshold was found to be an important and potentially limiting parameter for FLASH and should thus not be ignored in any future biological studies.

CONFLICT OF INTEREST

ACKNOWLEDGMENTS

DATA AVAILABILITY STATEMENT

Data sharing not applicable—the article describes entirely theoretical research.

REFERENCES

1. Favaudon V, Caplier L, Monceau V, et al. Ultrahigh dose-rate FLASH irradiation increases the differential response between normal and tumor tissue in mice. *Sci Transl Med*. 2014;6: 245ra93.
2. Montay-Gruel P, Bouchet A, Jaccard M, et al. X-rays can trigger the FLASH effect: ultra-high dose-rate synchrotron light source prevents normal brain injury after whole brain irradiation in mice. *Radiother Oncol*. 2018;129:582-588.
3. Hornsey S, Bewley DK. Hypoxia in mouse intestine induced by electron irradiation at high dose-rates. *Int J Radiat Biol Relat Stud Phys Chem Med*. 1971;19:479-483.
4. Montay-Gruel P, Petterson K, Jaccard M, et al. Irradiation in a flash: unique sparing of memory in mice after whole brain irradiation with dose rates above 100 Gy/s. *Radiother Oncol*. 2017;124:365-369.
5. Vozenin MC, Hendry JH, Limoli CL. Biological benefits of ultrahigh dose rate FLASH radiotherapy: sleeping beauty awoken. *Clin Oncol*. 2019;31:407-415.
6. Labarbe R, Hotoiu L, Barbier J, Favaudon V. A physicochemical model of reaction kinetics supports peroxyl radicalrecombination as the main determinant of the FLASH effect. *Radiother Oncol*. 2020;153:303-310.
7. Buonanno M, Grilj V, Brenner DJ. Biological effects in normal cells exposed to FLASH dose rate protons. *Radiother Oncol*. 2019;139:51-55.
8. Jin JY, Gu A, Wang W, Oleinick NL, Machtay M, Kong FMS. Ultra-high dose rate effect on circulating immune cells: a potentialmechanism for FLASH effect. *Radiother Oncol*. 2020;149:55-62.
9. Diffenderfer ES, Verginadis II, Kim MM, et al. Design, implementation and in vivo validation of a novel proton FLASH radiation therapy system. *Int J Radiat Oncol Biol Phys*. 2020;106(2):440-448.
10. Beyreuther E, Brand M, Hans S, et al. Feasibility of proton FLASH effect tested in zebrafish embryo irradiation. *Radiother Oncol*. 2019;139:46-50.
11. Bourhis J, Montay-Gruel P, Gonçalves Jorge P, et al. Clinical translation of FLASH radiotherapy: why and how? *Radiother Oncol*. 2019;139:11-17.
12. Van de Water S, Safai S, Schippers JM, Weber DC, Lomax AJ. Towards FLASH proton therapy: the impact of treatment planning and machine characteristics on achievable dose rates. *Acta Oncol*. 2019;58(12):1463-1469.
13. van Marlen P, Dahele M, Folkerts M, Abel E, Slotman BJ, Verbakel WFAR. Bringing FLASH to the clinic: treatment planning considerations for ultrahigh dose-rate proton beams. *Int J Radiat Oncol Biol Phys*. 2020;106(3):621-629.
14. Folkerts MM, Abel E, Busold S, Perez JR, Krishnamurthi V, Ling CC. A framework for defining FLASH dose rate for pencil beam scanning. *Med Phys*. 2020;47(12):6396-6404.
15. Mazal A, Prezado Y, Ares C, et al. FLASH and minibeams in radiation therapy: the effect of microstructures on time and space and their potential application to protontherapy. *Br J Radiol*. 2020;93:110720190807.
16. Pratx G, Kapp DS. A computational model of radiolytic oxygen-depletion during FLASH irradiation and its effecton the oxygen enhancement ratio. *Phys Med Biol*. 2019;64:185005.
17. Pedroni E, Bacher R, Blattmann H, et al. The 200-MeV proton therapy project at the Paul Scherrer Institute: conceptual design and practical realization. *Med Phys*. 1995;22(1):37-53.
18. Wieser HP, Cisternas E, Wahl N, et al. Development of the open-source dose calculation and optimization toolkit matRad. *Med Phys*. 2017;44(6):2556-2568.
19. Lomax A. Intensity modulation methods for proton radiotherapy. *Phys Med Biol*. 1999;44:185.
20. Van de Water S, Belosi MF, Albertini F, Winterhalter C, Weber DC, Lomax AJ. Shortening delivery times for intensity-modulated proton therapy by reducing the number of proton spots: and experimental verification. *Phys Med Biol*. 2020;65:095008.
21. Van de Water S, Kooy HM, Heijmen BJM, Hoogeman MS. Shortening delivery times of intensity modulated proton therapy by reducing proton energy layers during treatment plan optimization. *Int J Radiat Oncol Biol Phys*. 2015;92(2):460-468.
22. van Goethem MJ, van der Meer R, Reist HW, Schippers JM. Geant4 simulations of proton beam transport through a carbon or beryllium degrader and following a beam line. *Phys Med Biol*. 2009;54(19):5831-5846.
23. Rizzoglio V, Adelmann A, Baumgarten C. Evolution of a beam dynamics model for the transport line in a proton therapy facility. *Phys Rev Accel Beams*. 2017;20:124702. https://doi.org/10.1103/PhysRevAccelBeams.20.124702
24. Vozenin MC, de Fornel P, Petersson K, et al. The advantage of FLASH radiotherapy confirmed in mini-pig and cat-cancer patients. *Clin Cancer Res*. 2018;25(1):35-42. https://doi.org/10.1158/1078-0432.ccr-17-3375
25. Girdhani S, Jackson I, Eley J, et al. Characterization of radiation-induced lung fibrosis and mode of cell death using single and multi-pulsed proton flash irradiation. *Int J Radiat Oncol Biol Phys*. 2019;105:E652-E653.
26. Gao H, Lin J, Pratx, et al. Simultaneous dose and dose rate optimization (SDDRO) of the FLASH effect for pencil-beam-scanning

proton therapy. *Med Phys*. 2021. https://doi.org/10.1002/mp.15356

27. Gao H, Lin J, Lin Y, et al. Simultaneous dose and dose rate optimization (SDDRO) for FLASH proton therapy. *Med Phys*. 2020;47(12):6388-6395.

SUPPORTING INFORMATION

Additional supporting information may be found in the online version of the article at the publisher's website.